Theor. Comput. Fluid Dyn.
DOI 10.1007/s00162-013-0310-5

ORIGINAL ARTICLE

F. Lucci · V. S. L'vov · A. Ferrante · M. Rosso · S. Elghobashi

Eulerian–Lagrangian bridge for the energy and dissipation spectra in isotropic turbulence

Received: 31 May 2012 / Accepted: 11 July 2013

Abstract We study, numerically and analytically, the relationship between the Eulerian spectrum of kinetic energy, $E_{\rm E}(k,t)$, in isotropic turbulence and the corresponding Lagrangian frequency energy spectrum, $E_{\rm L}(\omega,t)$, for which we derive an evolution equation. Our DNS results show that not only $E_{\rm L}(\omega,t)$ but also the Lagrangian frequency spectrum of the dissipation rate $\varepsilon_{\rm L}(\omega,t)$ has its maximum at low frequencies (about the turnover frequency of energy-containing eddies) and decays exponentially at large frequencies ω (about a half of the Kolmogorov microscale frequency) for both stationary and decaying isotropic turbulence. Our main analytical result is the derivation of equations that *bridge* the Eulerian and Lagrangian spectra and allow the determination of the Lagrangian spectrum, $E_{\rm L}(\omega)$ for a given Eulerian spectrum, $E_{\rm E}(k)$, as well as the Lagrangian dissipation, $\varepsilon_{\rm L}(\omega)$, for a given Eulerian counterpart, $\varepsilon_{\rm E}(k)=2\nu k^2 E_{\rm E}(k)$. These equations were derived from the Navier–Stokes equations in the sweeping-free coordinate system (intermediate between the Eulerian and Lagrangian frameworks) which eliminates the effect of the kinematic sweeping of the small eddies by the larger eddies. We show that both analytical relationships between $E_{\rm L}(\omega)$ and $E_{\rm E}(k)$ and between $\varepsilon_{\rm L}(\omega)$ and $\varepsilon_{\rm E}(k)$ are in very good quantitative agreement with our DNS results and explain how $\varepsilon_{\rm L}(\omega,t)$ has its maximum at low frequencies and decays exponentially at large frequencies.

Keywords Eulerian-Lagrangian-bridge · Isotropic turbulence · Spectra

Communicated by S. Sarkar.

F. Lucci
Aerothermochemistry and Combustion Systems Laboratory,
ETH, Zürich, Switzerland

Present Address:
F. Lucci
Laboratory for I.C. Engines, EMPA, Dübendorf, Switzerland

V. S. L'vov
Department of Chemical Physics, The Weizmann Institute of Science,
76100 Rehovot, Israel

A. Ferrante
William E. Boeing Department of Aeronautics and Astronautics, University of Washington,
Seattle, WA 98195, USA

M. Rosso · S. Elghobashi (✉)
Department of Mechanical and Aerospace Engineering, University of California,
Irvine, CA 92697, USA
E-mail: selghoba@uci.edu

Published online: 24 July 2013

Contents

1 Introduction

A Lagrangian description of turbulence has unique physical advantages that are especially important in studies of phenomena dominated by small-scale motions or many-point correlation functions, like turbulent mixing and particle dispersion. As a result, a Lagrangian viewpoint following the motion of infinitesimal fluid elements is conceptually natural and practically useful for describing turbulent transport. Important early contributions include those of [20], (the displacement statistics for a single fluid particle) [19], (the relative-dispersion of a pair of particles) and [1] (the relative motion of particles). Later studies of turbulence from the Lagrangian viewpoint are those of [3,4,8,11,12,21,24] and references therein. Fundamental aspects and recent progress in investigating turbulence and turbulent mixing from a Lagrangian viewpoint (mostly experimental and numerical) are emphasized in a recent review by [24]. However, some important aspects of small-scale statistics, transport and other related phenomena, that can be studied via the Lagrangian approach, are still unclear or poorly understood. In particular, in a recent numerical study of the modulation of the turbulence kinetic energy (TKE) in decaying isotropic turbulence by dispersed inertial particles of the Taylor-length-scale size [13] showed that the *Eulerian* energy spectrum $E_E(t, k)$ suffers from oscillations at wavenumbers, k, corresponding to multiples of particle diameter. Our analysis showed that performing discrete Fourier transform of the Eulerian velocity field over the whole domain including the fluid volume occupied by the particles to compute $E_E(t, k)$ not only has limited physical meaning but also corrupts the spectrum at all the wavenumbers. As an alternative, we computed the *Lagrangian* energy frequency spectrum $E_L(t, \omega)$ of TKE from the autocorrelation function of the Lagrangian velocity $\boldsymbol{u}^L(\boldsymbol{x}_0|t)$ of a large number of fluid points. We then searched the literature for an evolution equation of $E_L(t, \omega)$, i.e., equation for $\frac{\partial}{\partial t} E_L(t, \omega)$, to study the effect of the dispersed particles on the individual terms in such equation. Our search indicated that an equation for $\frac{\partial}{\partial t} E_L(t, \omega)$ has not been reported in the available literature even for single-phase flows. In contrast, the equation for $\frac{\partial}{\partial t} E_E(t, k)$ is available in many papers and textbooks (e.g., [7] and [18]).

That search motivated the present study in which, as a preliminary step we derive, in Sect. 1, the equation for $\frac{\partial}{\partial t} E_L(t, \omega)$. Clearly, this equation has the same structure as that for $\frac{\partial}{\partial t} E_E(t, k)$, i.e., it includes the Lagrangian energy dissipation term $\varepsilon_L(t, \omega)$, instead of $\varepsilon_E(t, k)$, and Lagrangian energy transfer term instead of its Eulerian counterpart.

In Sect. 2, we present the results of direct numerical simulations (DNS) of stationary isotropic turbulence (in a cubical domain with 1024^3 mesh points and $Re_\lambda = 240$) and compare the Eulerian spectra $E_E(t, k)$ and $\varepsilon_E(t, k)$ with their Lagrangian counterparts $E_L(t, \omega)$ and $\varepsilon_L(t, \omega)$. The results show that $E_L(\omega)$ has a maximum at low frequencies (around the turnover frequency ω_0 of the energy-containing eddies) and decays at large ω, as $\sim 1/\omega^2$, as expected from Kolmogorov-41 (K41) dimensional reasoning for fully developed turbulence. Similarly, in this case, $E_E(k)$ decays at large k as $k^{-5/3}$, whereas $\varepsilon_E(k) \propto k^2 E_E(k)$ slowly increases as $\sim k^{1/3}$ at large k before its final decay. Thus, we initially expected that $\varepsilon_L(\omega)$ will also have a maximum at the inertial-dissipation crossover scale, i.e, near the turnover frequency ω_η of eddies of the Kolmogorov microscale η. However, our DNS results showed just the opposite: $\varepsilon_L(\omega)$ has a maximum around ω_0, then decays at large ω and practically vanishes around $\omega_\eta/2$.

This behavior of $\varepsilon_L(\omega)$ raised the central analytical question in this paper: "Could the Lagrangian spectra $E_L(\omega)$ and $\varepsilon_L(\omega)$ be determined from their Eulerian counterparts $E_E(k)$ and $\varepsilon_E(k)$"? Our answer is "Yes": In Sect. 3, we derive Eq. (24) that allow the determination of the Lagrangian (frequency) kinetic energy spectrum, $E_L(\omega)$, for a given Eulerian energy spectrum, $E_E(k)$, as well as the Lagrangian (frequency) dissipation spectrum, $\varepsilon_L(\omega)$, for a given Eulerian counterpart, $\varepsilon_E(k)$. These relationships are derived from the Navier–Stokes equations in the sweeping-free coordinate system (intermediate between the Eulerian and Lagrangian frameworks) which

eliminates the effect of the kinematic sweeping of the small eddies by the larger eddies. It is important to note that our derivation is *not* limited by either the inertial interval of scales, or by the requirement of large Re_λ and also does *not* include any empirical parameters. We demonstrate in Sect. 3 that both analytical relationships, $E_{\rm L}(\omega) \Leftrightarrow E_{\rm E}(k)$ and $\varepsilon_{\rm L}(\omega) \Leftrightarrow \varepsilon_{\rm E}(k)$, are in very good quantitative agreement with our DNS results.

We consider the *Eulerian–Lagrangian bridges* (24) and their agreement with our DNS as the central result of this paper and expect that they will shed light on the connections between the Eulerian and Lagrangian frameworks in turbulent flows.

2 Evolution equation of $E_{\rm L}(t, \omega)$

2.1 Lagrangian versus Eulerian equations of motion

In order to derive the balance equation of $E_{\rm L}(t, \omega)$ in the Lagrangian reference frame, we start from the non-dimensional Navier–Stokes equation for incompressible fluid in the Eulerian frame and use $\rho = 1$ as non-dimensional density:

$$\frac{{\rm D}u_i(\boldsymbol{x}, t)}{{\rm D}t} = -\frac{\partial p(\boldsymbol{x}, t)}{\partial x_i} + \frac{\partial \tau_{ij}(\boldsymbol{x}, t)}{\partial x_j} + f_i(\boldsymbol{x}, t), \tag{1a}$$

where

$$\frac{{\rm D}u_i(\boldsymbol{x}, t)}{{\rm D}t} = \frac{\partial u_i(\boldsymbol{x}, t)}{\partial t} + u_j(\boldsymbol{x}, t)\frac{\partial u_i(\boldsymbol{x}, t)}{\partial x_j}, \tag{1b}$$

is the material derivative, and τ_{ij} is the *viscous* stress tensor:

$$\tau_{ij}(\boldsymbol{x}, t) = \mu\left(\frac{\partial u_i(\boldsymbol{x}, t)}{\partial x_j} + \frac{\partial u_j(\boldsymbol{x}, t)}{\partial x_i}\right). \tag{1c}$$

The Lagrangian trajectory of a fluid point with initial position $\boldsymbol{x}_0$, at time $t = t_0$, is denoted as $\boldsymbol{x}^{\rm L} \equiv \boldsymbol{x}^{\rm L}(\boldsymbol{x}_0|t)$. By definition, $\boldsymbol{x}^{\rm L}(\boldsymbol{x}_0|t_0) = \boldsymbol{x}_0$. At time t, the fluid point passes through the position $\boldsymbol{x} = \boldsymbol{x}^{\rm L}(\boldsymbol{x}_0|t)$ with fluid point velocity $\boldsymbol{u}^{\rm L} \equiv \boldsymbol{u}^{\rm L}(\boldsymbol{x}_0|t)$:

$$\frac{{\rm d}\boldsymbol{x}^{\rm L}(\boldsymbol{x}_0|t)}{{\rm d}t} = \boldsymbol{u}\left(\boldsymbol{x}^{\rm L}(\boldsymbol{x}_0|t), t\right) \equiv \boldsymbol{u}^{\rm L}(\boldsymbol{x}_0|t). \tag{2a}$$

Similarly $f_i^{\rm L}$, $\left[\frac{\partial p}{\partial x_i}\right]^{\rm L}$ and $\nu\left[\frac{\partial^2 u_i}{\partial x_j \partial x_j}\right]^{\rm L}$ are the forcing, the pressure gradient and the viscous terms, respectively, along the fluid point trajectory, i.e., pathline. The notations $\boldsymbol{x}^{\rm L}(\boldsymbol{x}_0|t)$, etc. are used to emphasize that along a specific pathline, i.e., for a given $\boldsymbol{x}_0$, these quantities depend *only* on time t, and that $\boldsymbol{x}_0$ placed before the vertical line $(\boldsymbol{x}_0|\ldots)$ is the Lagrangian label (marker) which distinguishes the trajectories of different fluid points.

The Lagrangian "$[\ldots]^{\rm L}$" and the Eulerian flow variables are related according to:

$$f_i^{\rm L}(\boldsymbol{x}_0|t) = f_i\left(\boldsymbol{x}^{\rm L}(\boldsymbol{x}_0|t), t\right), \tag{2b}$$

$$\left[\frac{\partial p(\boldsymbol{x}_0|t)}{\partial x_i}\right]^{\rm L} = \frac{\partial p(\boldsymbol{x}, t)}{\partial x_i}\Big|_{\boldsymbol{x}=\boldsymbol{x}^{\rm L}(\boldsymbol{x}_0|t)}, \tag{2c}$$

$$\left[\frac{\partial^2 u_i(\boldsymbol{x}_0|t)}{\partial x_j \partial x_j}\right]^{\rm L} = \frac{\partial^2 u_i(\boldsymbol{x}, t)}{\partial x_j \partial x_j}\Big|_{\boldsymbol{x}=\boldsymbol{x}^{\rm L}(\boldsymbol{x}_0|t)}. \tag{2d}$$

The Lagrangian acceleration is defined as the time derivative of the Lagrangian velocity:

$$\frac{{\rm d}\boldsymbol{u}^{\rm L}(\boldsymbol{x}_0|t)}{{\rm d}t} = \frac{{\rm d}^2\boldsymbol{x}^{\rm L}(\boldsymbol{x}_0|t)}{{\rm d}t^2}, \tag{3a}$$

and is equal to the Lagrangian (or material) derivative of the Eulerian velocity $\frac{\mathrm{D}u_i(\boldsymbol{x},t)}{\mathrm{D}t}$ at the position $\boldsymbol{x} = \boldsymbol{x}^{\mathrm{L}}(\boldsymbol{x}_0|t)$:

$$\frac{\mathrm{d}\boldsymbol{u}^{\mathrm{L}}(\boldsymbol{x}_0|t)}{\mathrm{d}t} = \frac{\mathrm{D}u_i(\boldsymbol{x},t)}{\mathrm{D}t}\Big|_{\boldsymbol{x}=\boldsymbol{x}^{\mathrm{L}}(\boldsymbol{x}_0|t)}. \tag{3b}$$

The equality (3b) can be derived via Eqs. (1b), (2a) and (3a). Using Eq. (2), the Navier–Stokes Eq. (1a) can be written in terms of Lagrangian variables as

$$\frac{\mathrm{d}u_i^{\mathrm{L}}(\boldsymbol{x}_0|t)}{\mathrm{d}t} = -\left[\frac{\partial p(\boldsymbol{x}_0|t)}{\partial x_i}\right]^{\mathrm{L}} + \nu\left[\frac{\partial^2 u_i(\boldsymbol{x}_0|t)}{\partial x_j \partial x_j}\right]^{\mathrm{L}} + f_i^{\mathrm{L}}(\boldsymbol{x}_0|t). \tag{4}$$

2.2 Evolution equation for the Lagrangian energy frequency spectrum

In order to define the Lagrangian energy frequency spectrum, $E_{\mathrm{L}}(t,\omega)$, in the frequency domain, we first consider the autocorrelation function of the Lagrangian velocity $\boldsymbol{u}^{\mathrm{L}}(\boldsymbol{x}_0|t)$:

$$\Re^{\mathrm{L}}(t',t'') = \left\langle \boldsymbol{u}^{\mathrm{L}}(\boldsymbol{x}_0|t') \cdot \boldsymbol{u}^{\mathrm{L}}(\boldsymbol{x}_0|t'') \right\rangle_{\boldsymbol{x}_0}. \tag{5a}$$

Here, $\langle \ldots \rangle_{\boldsymbol{x}_0}$ denotes ensemble averaging over an infinite number of pathlines with different initial positions $\boldsymbol{x}_0$. Thus, in homogeneous turbulence, $\Re^{\mathrm{L}}(t',t'')$ is independent of the space coordinates (including $\boldsymbol{x}_0$). It should be noted that in decaying turbulence, $\Re^{\mathrm{L}}(t',t'')$ depends on both t' and t'', whereas in stationary (forced) turbulence, $\Re^{\mathrm{L}}(t',t'')$ depends only on the lag time $s = (t''-t')$.

We now express the independent variables t' and t'' in terms of (t) and (s) as $t' = t-(s/2)$ and $t'' = t+(s/2)$, where $t = (t'+t'')/2$ is the mean time, in order to redefine the autocorrelation $\mathcal{R}^L$ in terms of (t,s) in the form:

$$R^{\mathrm{L}}(t,s) = \Re^{\mathrm{L}}(t-(s/2), t+(s/2)) = \left\langle \boldsymbol{u}^{\mathrm{L}}(\boldsymbol{x}_0|t-s/2) \cdot \boldsymbol{u}^{\mathrm{L}}(\boldsymbol{x}_0|t+s/2) \right\rangle_{\boldsymbol{x}_0}. \tag{5b}$$

It should be noted that in homogeneous turbulence, the one-time, one-point Eulerian PDF is equal to the one-time, one-particle Lagrangian PDF [22]. Thus, for $s = 0$, $\frac{1}{2}R^{\mathrm{L}}(t,s)$ equals the TKE per unit mass, $E(t)$, and is expressed via Eulerian velocities as:

$$E(t) = E_{\mathrm{L}}(t) \equiv \frac{1}{2}\left\langle |\boldsymbol{u}^{\mathrm{L}}(\boldsymbol{x}_0|t)|^2 \right\rangle_{\boldsymbol{x}_0} = \frac{1}{2}R^{\mathrm{L}}(t,0), \tag{6}$$

where $\langle \ldots \rangle_{\boldsymbol{x}}$ denotes spacial averaging over Eulerian positions $\boldsymbol{x}$.

Now, we define $E_{\mathrm{L}}(t,\omega)$ as the Fourier transform of $\frac{1}{2}R^{\mathrm{L}}(t,s)$:

$$E_{\mathrm{L}}(t,\omega) = \frac{1}{2}\mathcal{F}\{R^{\mathrm{L}}(t,s)\}, \text{ where for a given generic function } \varphi(s) \text{ we have:} \tag{7a}$$

$$\mathcal{F}\{\varphi(s)\} \equiv \int_{-\infty}^{\infty} \varphi(s)\exp(i\omega s)\mathrm{d}s, \quad \text{and} \tag{7b}$$

$$\varphi(s) = \int_{-\infty}^{\infty} \mathcal{F}\{\varphi(s)\}\exp(-i\omega s)\frac{\mathrm{d}\omega}{2\pi}. \tag{7c}$$

Another definition of the Lagrangian energy frequency spectrum, $\widetilde{E}_{\mathrm{L}}(t,\omega) = \frac{1}{2}\mathcal{F}\{\Re^{\mathrm{L}}(t,t+s)\}$, is widely used in the literature. However, in decaying turbulence, this definition does not insure that all terms of the evolution equation Eq. (8a) are real since the symmetry of $\Re^{\mathrm{L}}$ is not guaranteed $\left(\Re^{\mathrm{L}}(t,t+s) \neq \Re^{\mathrm{L}}(t,t-s)\right)$.

In contrast, Eq. (7a) insures that all terms are real since according to the definition (5b), $R^{\mathrm{L}}(t,s) = R^{\mathrm{L}}(t,-s)$, and thus the $E_{\mathrm{L}}(t,\omega)$ spectrum is *real*.

It should be noted that $E_{\mathrm{L}}(t,\omega)$ is function of *two* variables and should be distinguished from $E_{\mathrm{L}}(t)$ which depends only on time. Note also that $E_{\mathrm{L}}(t)$ is the integral of the Lagrangian energy frequency spectrum $E_{\mathrm{L}}(t,\omega)$ with respect to ω, and with the factor $\frac{1}{2\pi}$.

The evolution equation for $E_{\mathrm{L}}(t,\omega)$ is derived by time-differentiating Eq. (7a), using the definitions (5) and the Lagrangian Navier–Stokes equations (LNS) (4). The result is:

$$\frac{\partial E_{\mathrm{L}}(t,\omega)}{\partial t} = \mathcal{T}_{\mathrm{L}}(t,\omega) - \varepsilon_{\mathrm{L}}(t,\omega) + \Psi_{\mathrm{L}}(t,\omega), \tag{8a}$$

where

$$\mathcal{T}_{\mathrm{L}}(t,\omega) = -\frac{1}{2}\mathcal{F}\left\langle u_i^{\mathrm{L}}\left(\boldsymbol{x}_0|t-\frac{s}{2}\right)\left[\frac{\partial p\left(\boldsymbol{x}_0|t+\frac{s}{2}\right)}{\partial x_i}\right]^{\mathrm{L}} + u_i^{\mathrm{L}}\left(\boldsymbol{x}_0|t+\frac{s}{2}\right)\left[\frac{\partial p\left(\boldsymbol{x}_0|t-\frac{s}{2}\right)}{\partial x_i}\right]^{\mathrm{L}}\right\rangle_{\boldsymbol{x}_0}, \tag{8b}$$

is the transfer rate of $E_{\mathrm{L}}(t,\omega)$ across the ω-space,

$$\varepsilon_{\mathrm{L}}(t,\omega) = -\frac{\nu}{2}\mathcal{F}\left\langle u_i^{\mathrm{L}}\left(\boldsymbol{x}_0|t-\frac{s}{2}\right)\left[\frac{\partial^2 u_i\left(\boldsymbol{x}_0|t+\frac{s}{2}\right)}{\partial x_j \partial x_j}\right]^{\mathrm{L}} + u_i^{\mathrm{L}}\left(\boldsymbol{x}_0|t+\frac{s}{2}\right)\left[\frac{\partial^2 u_i\left(\boldsymbol{x}_0|t-\frac{s}{2}\right)}{\partial x_j \partial x_j}\right]^{\mathrm{L}}\right\rangle_{\boldsymbol{x}_0}, \tag{8c}$$

is the viscous dissipation rate of $E_{\mathrm{L}}(t,\omega)$, and

$$\Psi_{\mathrm{L}}(t,\omega) = \frac{1}{2}\mathcal{F}\left\langle u_i^{\mathrm{L}}\left(\boldsymbol{x}_0|t-\frac{s}{2}\right) f_i^{\mathrm{L}}\left(\boldsymbol{x}_0|t+\frac{s}{2}\right) + u_i^{\mathrm{L}}\left(\boldsymbol{x}_0|t+\frac{s}{2}\right) f_i^{\mathrm{L}}\left(\boldsymbol{x}_0|t-\frac{s}{2}\right)\right\rangle_{\boldsymbol{x}_0}, \tag{8d}$$

is the rate of energy addition (via forcing) to $E_{\mathrm{L}}(t,\omega)$ to maintain turbulence stationarity. Details of this derivation are given in "Appendix A".

It should be noted that in the Eulerian frame, the transport equation of the kinetic energy spectrum $\mathrm{d}/\mathrm{d}t(E(k)) = \ldots$ shows that the rate of energy transfer between the different wave numbers is due to both the triple velocity correlation (originating from multiplying the nonlinear inertia terms of the Navier–Stokes equation by the velocity) and the correlation between the velocity and pressure gradient (see Hinze [7], Chapter 3). Note that the nonlinear velocity pressure gradient correlation effects are nonlocal. Now, in the Lagrangian frame, only the correlation between the velocity and pressure gradient [term (8b)] is responsible for the transfer of kinetic energy in the frequency space [see Eq. (4)]. A proof that the term (8b) is responsible for the transfer of energy between the different frequencies is that its integral over the frequency space vanishes as shown in Eq. (16) in the "Appendix".

3 Numerical procedure and results

Our DNS procedure is described in detail by [13], and thus, only the main parameters are given here. We use $1{,}024^3$ grid points in a cubical domain with periodic boundary conditions to simulate isotropic turbulent flow at $Re_\lambda = 240$ for a total dimensionless time $t = 50$ (about 20 eddy turnover times) and 102,400 time steps.

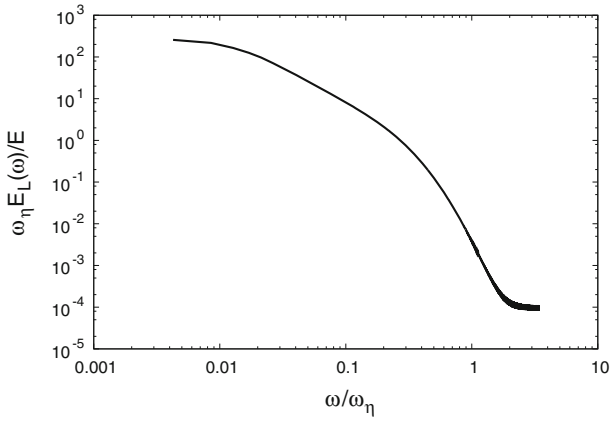

Fig. 1 Lagrangian energy frequency spectrum, $E_{\mathrm{L}}(\omega)$, for stationary isotropic turbulence

3.1 Stationary (forced) turbulence

In order to produce a stationary turbulence, we used Lundgren's linear forcing method [14] by applying a force $f_i(\boldsymbol{x}, t)$ proportional to the velocity in Eq. (1a) according to:

$$f_i(\boldsymbol{x}, t) = a(t) u_i(\boldsymbol{x}, t),$$

where $a(t)$ is the amplitude of the forcing and $\lfloor a(t) \rfloor = 1/\tau$. In this case, the balance equation for the TKE $E(t)$ is:

$$\frac{\mathrm{d}\, E(t)}{\mathrm{d}\, t} = -\varepsilon(t) + \frac{a(t)}{2} E(t), \tag{9a}$$

where $\varepsilon(t)$ is the viscous dissipation rate. For the prescribed amplitude $a(t) = 2\varepsilon(t)/E(t)$, Eq. (9a) gives:

$$\frac{\mathrm{d}\, E(t)}{\mathrm{d}\, t} = -\varepsilon(t) + \varepsilon(t) = 0. \tag{9b}$$

In order to obtain the Lagrangian energy frequency spectrum $E_{\mathrm{L}}(t, \omega)$, we compute the trajectories of 5×10^5 fluid points. These points are released at $t = 1$ randomly in the computational domain. The instantaneous Lagrangian velocity of the fluid point, required to integrate its trajectory, is computed using the fourth-order three-dimensional Hermite interpolation ("Appendix D" of [5]) from the fluid velocity at the eight Eulerian grid nodes surrounding the fluid point. The Lagrangian velocity of the fluid points is saved at time intervals $\Delta_{fp} t = 32 \Delta t$. The Lagrangian energy frequency spectrum $E_{\mathrm{L}}(t, \omega)$ is then obtained via the Fourier transform of the Lagrangian velocity autocorrelations according to (7a). Our DNS results for $E_{\mathrm{L}}(t, \omega)$ use the frequency ω_n defined as:

$$\omega_n = \frac{\pi n}{N_t \Delta_{fp} t}, \quad n = 1, \ldots, N_t, \tag{10}$$

where N_t is the total number of saved time steps. The frequencies ω_n are normalized by the Kolmogorov length-scale frequency $\omega_\eta = \pi/\tau_\eta = \pi\sqrt{\varepsilon/\nu}$, and ε is obtained by integrating the dissipation spectrum $\varepsilon_{\mathrm{L}}(\omega)$.

Figure 1 shows the Lagrangian energy frequency spectrum $E_{\mathrm{L}}(t, \omega)$ for stationary turbulence. Note that $E_L(\omega)$ is normalized via multiplying it by the quantity $\left(\omega_\eta / E\right)$ where $E = \int E_L(\omega) \mathrm{d}\omega$. The figure shows that the spectrum $E_{\mathrm{L}}(t, \omega)$ is similar to that in Fig. 3.23 in Pope's book [18]. The turnup at high frequencies $\omega/\omega_\eta > 2$ is due to numerical noise. It should also be noted that the time-dependence is not relevant in this case of stationary turbulence.

Figure 2 shows the frequency dependence of the three terms on the RHS of the evolution Eq. (8a), as well as their sum. Note that all terms are normalized by E. The figure shows that the sum of the three contributions, $\dfrac{\partial E_{\mathrm{L}}(t, \omega)}{\partial t}$, is zero as expected in stationary turbulence. All three terms have their maximum magnitude at the

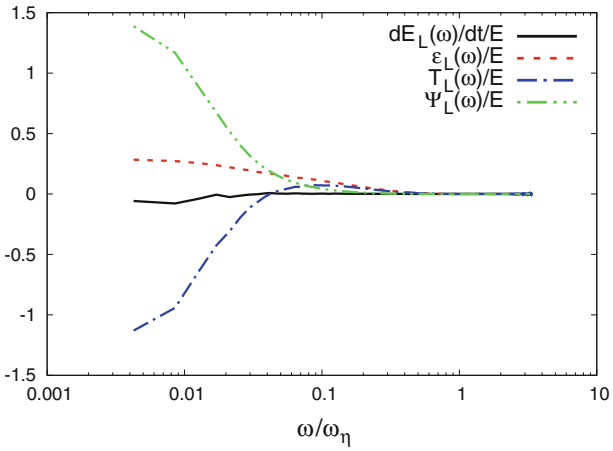

Fig. 2 Terms of the evolution equation (8) of $E_{\rm L}(t,\omega)$ for stationary isotropic turbulence

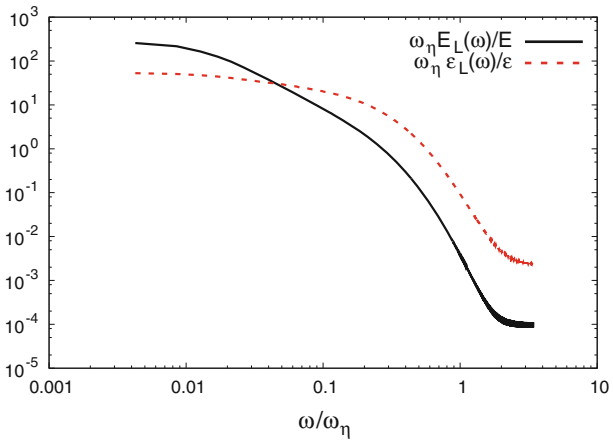

Fig. 3 Lagrangian frequency spectra of turbulence energy, $E_{\rm L}(\omega)$, and dissipation rate, $\varepsilon_{\rm L}(\omega)$, for stationary isotropic turbulence

lowest frequency. The energy transfer term $\mathcal{T}_{\rm L}(t,\omega)$ is negative at low frequencies and becomes positive for $\omega/\omega_\eta > 0.03$ indicating the transfer of TKE from the small to large frequency eddies.

The interesting result is that the dissipation rate $\varepsilon_{\rm L}(\omega)$ is maximum at low frequencies and decays exponentially at high frequencies, $\omega/\omega_\eta \gtrsim 0.5$.

Figure 3 shows the Lagrangian energy frequency spectrum, $E_{\rm L}(\omega)$, and the Lagrangian dissipation rate spectrum, $\varepsilon_{\rm L}(\omega)$, for stationary isotropic turbulence. Note that $\varepsilon_L(\omega)$ is normalized via multiplying it by the quantity $\left(\omega_\eta/\varepsilon\right)$ where $\varepsilon = \int \varepsilon_L(\omega)d\omega$. Again, the occurrence of the peak of $\varepsilon_{\rm L}(\omega)$ at low frequencies is clearly depicted and contrasts that of the Eulerian spectrum of the dissipation rate $\varepsilon(k)$ shown in Fig. 4 where the peak of $\varepsilon(k)$ occurs at high wavenumbers. This result will be discussed in Sect. 4. Our DNS results for decaying isotropic turbulence presented in the next subsection show the same behavior of $\varepsilon_{\rm L}(\omega)$ as in stationary turbulence.

3.2 Decaying isotropic turbulence

Here, we discuss the DNS results for $E_L(t,\omega)$ and the terms of the evolution Eq. (4) for decaying isotropic turbulence.

Figure 5 shows the frequency dependence of the three terms on the RHS of the evolution equation (4) as well as their sum. There is no forcing in this case, and thus the third term $\Psi_L(t,\omega) = 0$. The sum of the two remaining contributions, $\dfrac{\partial E_L(t,\omega)}{\partial t}$, is negative as expected for decaying turbulence.

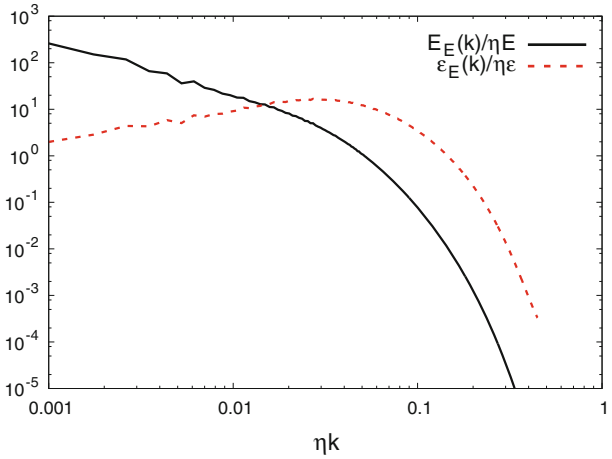

Fig. 4 Eulerian spectra of the energy $E_{\mathrm{E}}(k)$ and the dissipation rate $\varepsilon_{\mathrm{E}}(k)$ for stationary isotropic turbulence

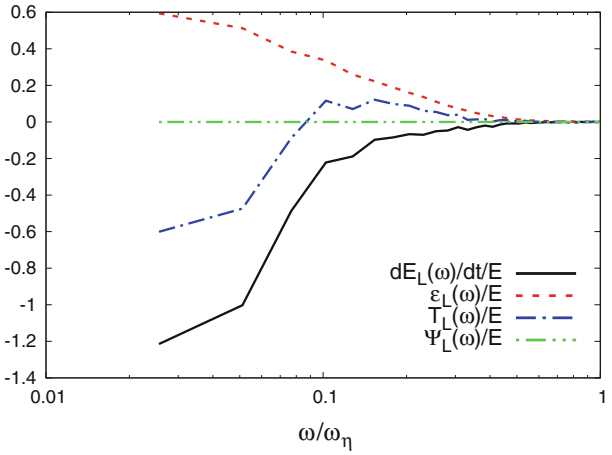

Fig. 5 Terms of the evolution equation (8) of $E_L(t, \omega)$ for decaying isotropic turbulence

Again, the dissipation rate $\varepsilon_L(t, \omega)$ is maximum at low frequencies and decays exponentially at high frequencies.

Figure 6 shows the Lagrangian energy frequency spectrum, $E_L(t, \omega)$, and the dissipation rate spectrum, $\varepsilon_L(t, \omega)$, for decaying isotropic turbulence. This result confirms that the unexpected maximum of $\varepsilon_L(t, w)$ at low frequencies (Fig. 6) is not an effect the stationarity or a side effect of the artificial forcing. The occurrence of the peak of $\varepsilon_L(t, \omega)$ at low frequencies will be discussed in the next section.

Note that the *Lagrangian frequency spectrum of the dissipation rate*, $\varepsilon_L(t, w)$, is the instantaneous rate of turbulence energy dissipation at a given frequency ω. The integral of $\varepsilon_L(t, w)$ over all frequencies is simply the instantaneous dissipation rate $\varepsilon(t)$ at time t.

4 Analytical description of the frequency spectra $E_{\mathrm{L}}(\omega)$ and $\varepsilon_{\mathrm{L}}(\omega)$ and its comparison with DNS

In order to explain why $\varepsilon_{\mathrm{L}}(\omega)$ is maximum at low frequencies, we need to examine *analytically, based on Navier–Stokes equations*, the interactions between the *small scale* eddies which are the main contributors to $\varepsilon_{\mathrm{L}}(\omega)$. The difficulty in this approach is that the statistical description of the energy exchange between the different turbulent eddies involves different time-correlation functions of the velocity field [10,16,23]. The balance equation of the turbulence energy in the inertial range involves the second-order (two-point, two-time) correlation in the Eulerian framework is

$$W_{ij}^{\mathrm{E}}(\mathbf{r}, \mathbf{r}', t, t') = \left\langle u_i(\mathbf{r}, t) u_j(\mathbf{r}', t') \right\rangle. \tag{11}$$

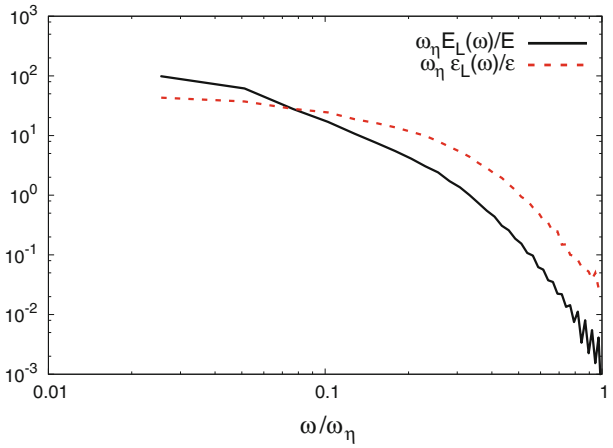

Fig. 6 Lagrangian energy frequency spectrum, $E_L(t,\omega)$, and dissipation spectrum, $\varepsilon_L(t,\omega)$, for decaying isotropic turbulence

However, $W_{ij}^{\mathrm{E}}(\mathbf{r},\mathbf{r}',t,t')$ is not universal because its time-dependence is determined by contributions to $\boldsymbol{u}(\mathbf{r},t)$ from the largest scales which are controlled by the energy input mechanisms.

To clarify this issue, consider a turbulent flow that consists only of large eddies of scale L in the energy-containing range and small eddies of scale $l \ll L$, in the inertial subrange (see Fig. 7A). According to the K41 scaling [9], the velocity of the small eddies, v_l, is related to the velocity of large eddies as $v_l \sim V_L(l/L)^{1/3} \ll V_L$, and the turnover time of the small eddies $\tau_l \sim l/v_l \sim \tau_L(l/L)^{2/3} \ll \tau_L$, where $\tau_L \sim L/V_L$ is the turnover time of large eddies.

Figure 7B shows a magnified view of the two small eddies, of size $l \ll L$, in the dotted square of Fig. 7A, with their velocity field described in the Eulerian coordinate system XYZ. The centers of these two eddies are located at $\boldsymbol{r}_0$ and $\boldsymbol{r}_1$ at time t_0 as shown by black solid lines. Since $v_l \ll V_L$, the total velocity field is dominated by the motion of the large eddy and thus can be considered as homogeneous field at scales $l \ll L$. This velocity field advects the small eddies a distance $\approx l$ during the "sweeping time" $T_l \sim l/V_L$ which is much shorter than their life time $\tau_l \sim l/v_l$. Accordingly, the small eddies shape and size remain unchanged after being swept to the new positions $\boldsymbol{r}_{0\delta}$ and $\boldsymbol{r}_{1\delta}$ as shown by dashed lines in Fig. 7B.

The above description leads to the following conclusions:

1. The two-point Eulerian correlation function with separation $|\boldsymbol{r}-\boldsymbol{r}'| \sim l$ decays with the characteristic sweeping time T_l. This is because during the time T_l, one small eddy of scale l is replaced by another eddy of the same scale with uncorrelated velocity field.
2. The shape and energy of l-eddies remain almost unchanged during the sweeping time T_l. Therefore, in the Eulerian description, the dynamical interactions between the l-eddies during their lifetime is practically invisible due to the sweeping effect.

Thus, the nonlinear (inertia) terms of ENS (1) cause the *kinematic sweeping* of small eddies by the velocity field of the largest eddies, in addition to the *dynamical interaction* between the different modes (e.g., vortex stretching). This *kinematic sweeping*, with the characteristic frequency $1/T_l$, preserves the shapes of the advected small-scale eddies and thus has no effect on the turbulence energy spectrum in the Eulerian frame. Only the much smaller *dynamical* interactions between the small eddies (with the characteristic frequency $1/\tau_l$) affect the spectrum of turbulence energy. Thus, the masking effect of the kinematic sweeping makes it difficult to perform a rigorous *analytical* description of turbulence in the Eulerian frame.

For example, [10] in his direct-interaction approximation (DIA) obtained the spectrum $E_{\mathrm{E}}(k) \propto k^{-3/2}$ which obviously contradicts the generally accepted K41 prediction $E_{\mathrm{E}}(k) \propto k^{-5/3}$.

A potentially promising approach is to recast the Navier–Stokes equation in terms of Lagrangian coordinates as has been attempted by [11]. In this approach, illustrated in Fig. 7C, the Lagrangian velocity, $\boldsymbol{u}^{\mathrm{L}}(\boldsymbol{x}|t)$, is defined for each fluid point with respect to its *individual* reference frame whose origin $\boldsymbol{x}^{\mathrm{L}}(\boldsymbol{x},t)$ is moving with velocity:

$$\boldsymbol{u}^{\mathrm{L}}(\boldsymbol{x}|t) \equiv \boldsymbol{u}\left(\boldsymbol{x}^{\mathrm{L}}(\boldsymbol{x},t),t\right). \tag{12}$$

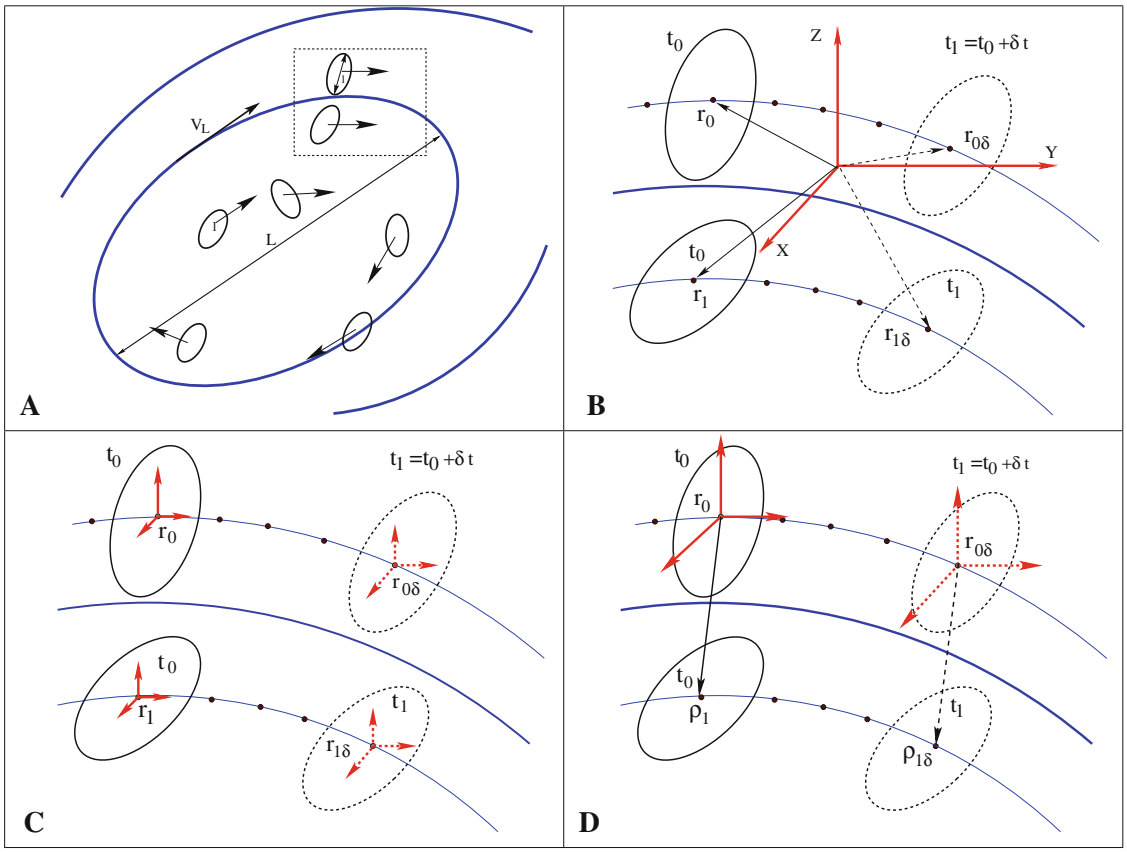

Fig. 7 Panel A: Schematic of a typical large eddy of scale L in a turbulent flow; the streamlines are shown in *blue lines* with the characteristic velocity V_L; small eddies of scale $l \ll L$ shown as *black streamlines* with velocities $\sim v_l \ll V_L$ are being advected by the velocity field of the large eddy. Panels B,C and D show a magnified view of the two small eddies in the *dotted square* in panel A with their velocity field described in different coordinate systems. Panel B shows an Eulerian coordinate system, XYZ, in which the positions of the fluid points $\boldsymbol{r}_j$ are measured with reference to this inertial frame. Also shown are the trajectories of two fluid points located initially at $\boldsymbol{r}_0$ and $\boldsymbol{r}_1$ (shown by *black solid arrows*) at time t_0 and later at $\boldsymbol{r}_{0\delta}$ and $\boldsymbol{r}_{1\delta}$ (shown by *black dashed arrows*) at time $t_1 = t_0 + \delta t$. Panel C provides a Lagrangian description of the flow in which every fluid point has its "own" reference frame whose origin coincides always with the moving fluid point. Only two such frames are shown, associated with the two fluid points $\boldsymbol{r}_0$ and $\boldsymbol{r}_1$ at $t = t_0$ (*red solid arrows*); the origins of the two frames moved to the positions $\boldsymbol{r}_{0\delta}$ and $\boldsymbol{r}_{1\delta}$ at $t = t_1$ (shown by *red dashed arrows*). Panel D illustrates the Belinicher–L'vov (BL) description of the flow in which there is *only one reference frame* (shown in *red*) whose origin is moving always with O-point ($\boldsymbol{r}_0$ at t_0 and $\boldsymbol{r}_{0\delta}$ at t_1). Any small region of size l within the large eddy *"sees"* an almost homogenous mean-velocity field which is eliminated in the BL-frame. Only the velocity field of the small-scale eddies is retained in the BL-frame (color figure online)

Figure 7C shows a Lagrangian reference frame for only two fluid points, located at $\boldsymbol{r}_0$ and $\boldsymbol{r}_1$ at time t_0 (red solid arrows) and moved along the streamlines to points $\boldsymbol{r}_{0\delta}$ and $\boldsymbol{r}_{1\delta}$ at time $t_1 = t_0 + \delta t$ (red dashed arrows). It should be noted that in these co-moving frames, the sweeping effect is absent. The Lagrangian velocities are strongly correlated at the sweeping time, T_l, and the Lagrangian two-point correlation function W_{ij}^{L} [similar to W_{ij}^{E}, given by Eq. (11)] will decay with characteristic time τ_l, indicating the dynamical effects of energy exchange between eddies of comparable small scales. Kraichnan [11] obtained energy frequency spectra for passive scalar diffusion, two- and three-dimensional turbulence, and Burgers dynamics. However, the resulting Lagrangian-history DIA [11] is extremely cumbersome mainly because the LNS (4) includes at time t the entire history of the velocity field for times $0 < t' < t$ implicitly through the Lagrangian trajectories $\boldsymbol{x}^{\mathrm{L}}(\boldsymbol{x}_0|t)$, i.e., via complicated nonlinear time evolution operators. Consequently, the right-hand side of Eq. (8a) depends on the dynamical quantities (8b), (8c) and (8d) which can be evaluated only numerically from DNS. This is the reason that little progress has been made in the analytical description of the statistics of turbulence in the Lagrangian frame.

Another approach is due to [2], hereinafter referred to as BL, who suggested to *eliminate the kinematic sweeping effect* on the small-scale motion by using a reference frame shared by *all* fluid points inside a large eddy as shown in Fig. 7D. The origin of this frame always moves along the Lagrangian trajectory $\boldsymbol{x}^{\mathrm{L}}(\boldsymbol{x}_0|t)$ of a particular fluid point, denoted as O-point, with position $\boldsymbol{x}_0$ at time $t = t_0$. Monin [17] used the same coordinate system to extend the region of validity of the well-known Kolmogorov's relation between the second-order and third-order structure functions. For eddies that are statistically important for the energy flux over scale $l \ll L$ ($l \approx$ the distance between fluid points and the O-point) and during times $\tau_l \ll \tau_L$, the difference between Lagrangian and BL-velocities is small. Accordingly, the sweeping effect in the BL approach is absent as in the Lagrangian approach. However, the *crucial advantage* of the BL over the Lagrangian approach is that the resulting BL-equation of motion (19) is of the same form as ENS and does not involve the history of the velocity field. The BL-equation allows the derivation (in "Appendix B") of the following bridging equations:

$$E_{\mathrm{L}}(\omega) \simeq 2\pi \int \exp\left[-\frac{\omega}{\gamma(k)}\right] \frac{E_{\mathrm{E}}(k)\,\mathrm{d}k}{\gamma(k)}, \qquad \text{Bridge for energy spectra;} \tag{13a}$$

$$\frac{\varepsilon_{\mathrm{L}}(\omega)}{2\,\nu} \simeq 2\pi \int \exp\left[-\frac{\omega}{\gamma(k)}\right] \frac{k^2 E_{\mathrm{E}}(k)\,\mathrm{d}k}{\gamma(k)}, \qquad \text{Bridge for dissipation spectra.} \tag{13b}$$

Equations (13a) and (13b) are the *main theoretical result in this paper. Equation* (13a) *allows the determination of the Lagrangian (frequency) kinetic energy spectrum* $E_{\mathrm{L}}(\omega)$*, for a given Eulerian energy spectrum* $E_{\mathrm{E}}(k)$*. Similarly, Eq.* (13b) *provides the Lagrangian (frequency) dissipation spectrum* $\varepsilon_{\mathrm{L}}(\omega)$*, for a given Eulerian counterpart* $\varepsilon_{\mathrm{E}}(k) = 2\nu k^2 E(k)$*. It is important to note that the Eulerian–Lagrangian bridges* (13) *are not limited by either the inertial interval of scales, or by the requirement of large* Re_λ*.*

For large Re_λ in the inertial integral of scales, the bridge relationships (13) can be further simplified using the facts that:

(1) The integrand in Eqs. (13) decays fast enough in the region where $\gamma(k) < \omega$, and
(2) $\gamma(k) \simeq \varepsilon^{1/3} k^{2/3}$.

Introducing $k(\omega) \equiv \sqrt{\omega^3/\varepsilon}$, we can approximate the integrals in (13a) and (13b) via replacing the zero lower limit by $k(\omega)$, and the upper limit by $(1/\eta)$, the reciprocal of the Kolmogorov length scale. The new integration limits describe a range of frequencies where $\gamma(k) > \omega$, i.e., $\Phi[\omega/\gamma(k)] \simeq 1$ as shown below:

$$E_{\mathrm{L}}(\omega) \simeq \int_{k(\omega)}^{1/\eta} \frac{E_{\mathrm{E}}(k)\,\mathrm{d}k}{\gamma(k)} \simeq \varepsilon^{1/3} \int_{k(\omega)}^{1/\eta} \frac{\mathrm{d}k}{k^{7/3}} \simeq -\frac{\varepsilon^{1/3}}{k^{4/3}}\bigg|_{k(\omega)}^{1/\eta} \simeq \varepsilon\left(\frac{1}{\omega^2} - \frac{1}{\omega_\eta^2}\right), \tag{14a}$$

$$\frac{\varepsilon_{\mathrm{L}}(\omega)}{\nu} \simeq \int_{k(\omega)}^{1/\eta} \frac{k^2 E_{\mathrm{E}}(k)\,\mathrm{d}k}{\gamma(k)} \simeq \varepsilon^{1/3} \int_{k(\omega)}^{1/\eta} \frac{\mathrm{d}k}{k^{1/3}} \simeq \varepsilon^{1/3} k^{2/3}\Big|_{k(\omega)}^{1/\eta} \simeq \left(\omega_\eta - \omega\right), \tag{14b}$$

where $\omega_\eta = \pi\sqrt{\varepsilon/\nu}$ is the turnover frequency of the Kolmogorov-scale eddies. Equation (14a) shows that for $\omega \ll \omega_\eta$, the integral is dominated by its lower limit, $k \simeq k(\omega)$. This result can be considered as a *locality assumption, which* is valid for $E_{\mathrm{L}}(\omega)$. Accordingly, in this region $E_{\mathrm{L}}(\omega) \simeq \varepsilon/\omega^2$ in agreement with the naïve K41 dimensional reasoning. The dependence $E_{\mathrm{L}}(\omega) \simeq \varepsilon/\omega^2$ is shown in Fig. 8 by the black straight line of slope $= -2$. As ω approaches ω_η, the right-hand side of Eq. (14a) shows that $E_{\mathrm{L}}(\omega)$ diminishes and deviates from the straight line in agreement with the DNS results in Fig. 8.

Regarding the Lagrangian dissipation, $\varepsilon_{\mathrm{L}}(\omega)$, we have derived the result (14b) which shows that $\varepsilon_{\mathrm{L}}(\omega)$ is maximum at small values of ω in agreement with our DNS result (Figs. 2 and 3). This is in contrast to the result of the *naïve* K41 dimensional reasoning that gives just the opposite behavior $\varepsilon_{\mathrm{L}}(\omega) \sim \nu\omega$.

The result (14b) follows from the fact that the main contribution to $\varepsilon_{\mathrm{L}}(\omega)$ comes from the turbulent motions with $k \gtrsim k(\omega)$ but smaller than $1/\eta$. In fact, the integral in Eq. (14b) is $\propto k^{2/3}$, thus it is dominated by its *upper limit* $1/\eta$, and therefore the locality assumption $k \simeq k(\omega)$ is invalid for the evaluation of $\varepsilon_{\mathrm{L}}(\omega)$.

Figures 8 and 9 compare the DNS results with the analytically predicted Lagrangian energy frequency spectrum $E_{\mathrm{L}}(\omega)$ and the Lagrangian spectrum of the dissipation rate $\varepsilon_{\mathrm{L}}(\omega)$. Since the numerical prefactors were not included in the analytical model equations (24), we normalized $E_{\mathrm{L}}(\omega)$ and $\varepsilon_{\mathrm{L}}(\omega)$ by (E/ω_η) and $(\varepsilon/\omega_\eta)$ respectively as was done in the previous figures. The dashed lines in both figures denote the analytical solutions via Eq. (13) in which the values of the Eulerian k-spectrum, $E_{\mathrm{E}}(k)$ were obtained from our DNS

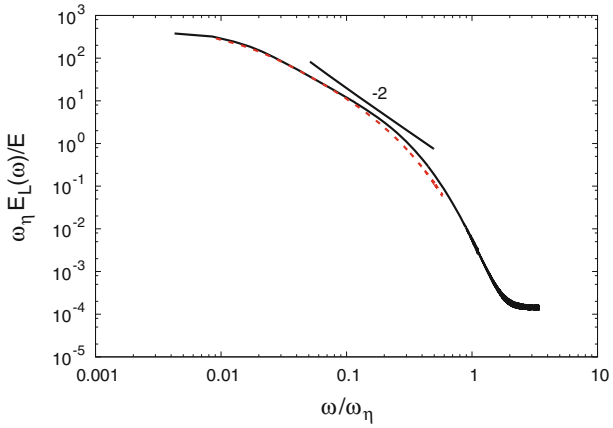

Fig. 8 Lagrangian energy frequency spectrum, $E_{\rm L}(\omega)$, for stationary isotropic turbulence. *Solid line* DNS; *dashed line* Eq. (24a) with Φ evaluated from Eq. (23b) and $E(k)$ from Fig. 4. The data of the *dashed line* ($0.01 \leq \omega/\omega_\eta \leq 0.6$) are limited by the available DNS data. The *straight line* with slope -2 represents the K41 estimate of $E_L(\omega) \propto \omega^{-2}$

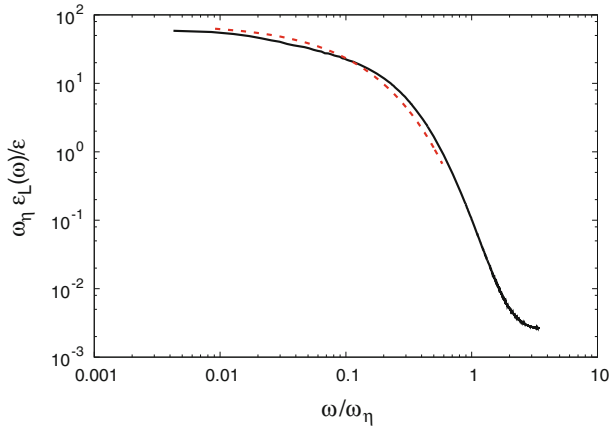

Fig. 9 Lagrangian dissipation spectrum, $\varepsilon_{\rm L}(\omega)$, for stationary isotropic turbulence. *Solid line* DNS; *dashed line* Eq. (24b) with Φ evaluated from Eq. (23b) and $E(k)$ from Fig. 4. The data of the *dashed line* ($0.01 \leq \omega/\omega_\eta \leq 0.6$) are limited by the available DNS data

results. Then we performed the integration in Eq. (13) numerically. The agreement between the analytical model (13), and the DNS results is very good for both $E_{\rm L}(\omega)$ and $\varepsilon_{\rm L}(\omega)$. We conclude that the our analytical model (13) reproduces our DNS results.

It is important to note that our main analytical result, Eq. (13), and the estimates (14) are not based on some "physical picture" of turbulent motions, but formally follow from the NS equation in the sweeping-free BL representation which is an exact transformation of variables.

5 Concluding remarks

We presented DNS results of the Lagrangian frequency spectra of the TKE, $E_{\rm L}(t,\omega)$ and its dissipation rate $\varepsilon_{\rm L}(t,\omega)$ in stationary homogeneous isotropic turbulence. The Eulerian velocity field was computed at $Re_\lambda = 240$ in a cubical domain containing $1{,}024^3$ mesh points. The Lagrangian velocity autocorrelations of 4×10^5 fluid points were used to obtain the Lagrangian frequency spectra.

Our DNS results show that not only $E_{\rm L}(t,\omega)$ but also $\varepsilon_{\rm L}(t,\omega)$ has its maximum at low frequencies ω (about the turnover frequency of energy-containing eddies) and decays exponentially at large ω (about a half of the Kolmogorov microscale frequency) for both stationary and decaying isotropic turbulence.

Our main analytical result is the derivation of Eulerian–Lagrangian bridge relationships (13) and the estimates (14) that allow the determination $E_{\rm L}(t,\omega)$ and $\varepsilon_{\rm L}(t,\omega)$ in terms of their Eulerian counterparts: the spectra of energy $E_{\rm E}(t,k)$ and dissipation rate $\varepsilon_{\rm E}(t,k)$ in 1-dimensional k-space.

These relationships were derived from the Navier–Stokes equations in the sweeping-free Belinicher–L'vov (BL) representation (intermediate between Eulerian and Lagrangian frameworks) which eliminates the effect of the kinematic sweeping of the small eddies by the larger eddies. This kinematic sweeping is an inherent action of the nonlinear (advection) terms of Navier–Stokes equation in Eulerian coordinates, and thus precludes the analytical study of the *small-scale interactions*. In contrast, the BL representation allows the examination of the interaction between the small-scale motions. The derivation of the bridge relationships was achieved via the combined (k, ω) energy spectrum $E_{\mathrm{BL}}(t, k, \omega)$. The integration of $E_{\mathrm{BL}}(t, k, \omega)$ with respect to ω gives $E_{\mathrm{E}}(t, k)$, while the k-integral gives $E_{\mathrm{L}}(t, \omega)$.

We demonstrate that both analytical relationships, $E_{\mathrm{L}}(\omega) \Leftrightarrow E_{\mathrm{E}}(k)$ and $\varepsilon_{\mathrm{L}}(\omega) \Leftrightarrow \varepsilon_{\mathrm{E}}(k)$, are in very good quantitative agreement with our DNS results without any empirical parameters.

Acknowledgments The computations were performed on the Blue Gene/P at Argonne National Laboratory through a US Department of Energy ASCR/ALCC award to the corresponding author (SE). S.E. and V.L. acknowledge the partial support for this research by the US-Israel Binational Science Foundation. A.F. acknowledges support by the National Science Foundation CAREER Award (OCI-1054591).

Appendix A

Derivation of the evolution equation of $E_{\mathrm{L}}(t, \omega)$

In order to derive an evolution equation for $E_{\mathrm{L}}(t, \omega)$, we start from Eq. (7a) which gives:

$$\frac{\partial E_{\mathrm{L}}(t,\omega)}{\partial t} = \frac{\partial}{2\partial t}\mathcal{F}\{R^{\mathrm{L}}(t,s)\} = \mathcal{F}\left\{\frac{\partial R^{\mathrm{L}}(t,s)}{2\partial t}\right\}. \tag{15a}$$

We use the definition of $\dfrac{\partial R^{\mathrm{L}}(t,s)}{\partial t}$ in (5b) and the fact that two independent linear operations (time differentiation and ensemble averaging $\langle \dots \rangle_{\boldsymbol{x}_0}$) can be commuted to obtain:

$$\begin{aligned}\frac{\partial R^{\mathrm{L}}(t,s)}{\partial t} = &\left\langle \boldsymbol{u}^{\mathrm{L}}(\boldsymbol{x}_0|t-s/2)\cdot\frac{\mathrm{d}\boldsymbol{u}^{\mathrm{L}}(\boldsymbol{x}_0|t+s/2)}{\mathrm{d}t}\right\rangle_{\boldsymbol{x}_0}\\ &+\left\langle \boldsymbol{u}^{\mathrm{L}}(\boldsymbol{x}_0|t+s/2)\cdot\frac{\mathrm{d}\boldsymbol{u}^{\mathrm{L}}(\boldsymbol{x}_0|t-s/2)}{\mathrm{d}t}\right\rangle_{\boldsymbol{x}_0}.\end{aligned} \tag{15b}$$

We now substitute the time derivatives $\mathrm{d}\boldsymbol{u}^{\mathrm{L}}/\mathrm{d}t$ in Eq. (15b) with the RHS of Eq. (4), expressed at the two different times $(t + s/2)$ and $(t - s/2)$. Finally, we perform the Fourier transform to obtain the evolution Eq. (8) for $E_{\mathrm{L}}(t, \omega)$. Note that all the terms on the RHS of Eqs. (8a), (8b), (8c) and (8d) are real and even functions of ω. Furthermore, the integral of the energy transfer term (8b) with respect to frequency equals zero, as expected. The proof is as follows.

$$\int_{-\infty}^{\infty}\mathcal{T}_{\mathrm{L}}(t,\omega)\frac{d\omega}{2\pi} = -\left\langle u_i^{\mathrm{L}}(\boldsymbol{x}_0|t)\left[\frac{\partial p(\boldsymbol{x}_0|t)}{\partial x_i}\right]^{\mathrm{L}}\right\rangle \tag{16a}$$

$$= -\left\langle u_i(\boldsymbol{x},t)\left[\frac{\partial p(\boldsymbol{x},t)}{\partial x_i}\right]\right\rangle \tag{16b}$$

$$= \left\langle\left[\frac{\partial u_i(\boldsymbol{x},t)}{\partial x_i}\right]p(\boldsymbol{x},t)\right\rangle = 0 \tag{16c}$$

where the RHS of Eq. (16a) is obtained by using Eq. (7c) with $s = 0$, i.e., $\int\tilde{\varphi}(\omega)d\omega/2\pi = \varphi(0)$, in which $\tilde{\varphi}(\omega)$ represents $\mathcal{T}_{\mathrm{L}}(t, \omega)$. Equation (16b) follows from the definition (6) for the velocity and other Lagrangian quantities, i.e., the one-time, one-particle ($s = 0$) Lagrangian correlation function is identical to the corresponding one-time, one-point Eulerian correlation. Equation (16c) is based on the homogeneous

turbulence property: $\left\langle \frac{\partial [A(\boldsymbol{x})B(\boldsymbol{x})]}{\partial x_i} \right\rangle = 0$, which gives $\left\langle A(\boldsymbol{x}) \frac{\partial B(\boldsymbol{x})}{\partial x_i} \right\rangle = -\left\langle B(\boldsymbol{x}) \frac{\partial A(\boldsymbol{x})}{\partial x_i} \right\rangle$ for any two random functions $A(\boldsymbol{x})$ and $B(\boldsymbol{x})$. Equation (16c) is a result of the incompressibility condition.

Appendix B

Derivation of the bridge relations (13) using the sweeping-free BL approach

Following [2], we define the BL-velocity, $\boldsymbol{u}^{\mathrm{BL}}(\boldsymbol{x}_0|\boldsymbol{x}, t)$, as the Eulerian velocity $\boldsymbol{u}$ in the *shared* reference frame:

$$\boldsymbol{u}^{\mathrm{BL}}(\boldsymbol{x}_0|\boldsymbol{x}, t) \equiv \boldsymbol{u}\left(\boldsymbol{x} - \boldsymbol{x}_0 + \boldsymbol{x}^{\mathrm{L}}(\boldsymbol{x}_0, t), t\right). \tag{17}$$

The turbulent flow properties in the vicinity of the O-point are then described by rewriting the ENS equation (1) in this shared reference frame. In contrast, the Lagrangian velocity, $\boldsymbol{u}^{\mathrm{L}}(\boldsymbol{x}|t)$, is defined for each fluid point with respect to its *individual* reference frame whose origin $\boldsymbol{x}^{\mathrm{L}}(\boldsymbol{x}, t)$ is moving with velocity $\boldsymbol{u}(\boldsymbol{x}^{\mathrm{L}}(\boldsymbol{x}, t), t)$.

It should be noted that the BL approach is *not* an approximation, but an *exact* coordinate transformation. The recent review by [6] provides more details about the elimination of the sweeping effects and the BL approach.

Accordingly, the ENS (1) for time t in the BL-coordinates (BLNS), derived by [2] includes *only* the BL-velocity field at the same time t. Formally, the BLNS equation has the form of (1) but with the replacement $u_i(\boldsymbol{x}, t) \Rightarrow u_i^{\mathrm{BL}}(\boldsymbol{x}_0|\boldsymbol{x}, t)$, and

$$\frac{\mathrm{D}}{\mathrm{D}t} = \left\{ \frac{\partial}{\partial t} + u_j(\boldsymbol{x}, t) \frac{\partial}{\partial x_j} \right\} \Rightarrow \frac{\mathrm{D}^{\mathrm{BL}}}{\mathrm{D}t} = \left\{ \frac{\partial}{\partial t} + \left[u_j^{\mathrm{BL}}(\boldsymbol{x}_0|\boldsymbol{x}, t) - u_j^{\mathrm{BL}}(\boldsymbol{x}_0|\boldsymbol{x}_0, t) \right] \frac{\partial}{\partial x_j} \right\}. \tag{18}$$

The resulting BLNS equation is:

$$\frac{\mathrm{D}^{\mathrm{BL}} u_i^{\mathrm{BL}}(\boldsymbol{x}_0|\boldsymbol{x}, t)}{\mathrm{D}t} = -\frac{\partial p^{\mathrm{BL}}(\boldsymbol{x}_0|\boldsymbol{x}, t)}{\partial x_i} + \frac{\partial \tau_{ij}^{\mathrm{BL}}(\boldsymbol{x}_0|\boldsymbol{x}, t)}{\partial x_j} + f_i^{\mathrm{BL}}(\boldsymbol{x}_0|\boldsymbol{x}, t), \tag{19}$$

Note that both the BLNS (19) and ENS (1) do not involve the history of the fluid points trajectories, whereas LNS (4) does. However, the kinematic sweeping effect, inherent in the ENS, is eliminated from Eq. (19) because the large-scale eddies do not contribute to the BL-velocity difference $\left[u_j^{\mathrm{BL}}(\boldsymbol{x}_0|\boldsymbol{x}, t) - u_j^{\mathrm{BL}}(\boldsymbol{x}_0|\boldsymbol{x}_0, t) \right]$, in contrast to the ENS as shown in [2]. Therefore, the BLNS (19) is ideal for our theoretical study.

The main contribution to the two-point ($\boldsymbol{r}'$ and $\boldsymbol{r}''$), different-time (t' and t'') velocity correlation function (with $\boldsymbol{r}' + \boldsymbol{r}'' = 2\boldsymbol{r}_0$ and $t' + t'' = 2t_0$) originates from the vicinity of the trajectory $(\boldsymbol{x}^{\mathrm{L}}(\boldsymbol{x}_0, t), t)$, where the difference between BL- and L-velocities can be neglected. Thus, the two-point, different-time cross-velocity correlation of the BL-velocities in homogeneous turbulence is written as:

$$W(\boldsymbol{x}, s) \equiv \left\langle \boldsymbol{u}^{\mathrm{BL}}(\boldsymbol{x}_0|\boldsymbol{x}', t') \cdot \boldsymbol{u}^{\mathrm{BL}}(\boldsymbol{x}_0|\boldsymbol{x}'', t'') \right\rangle, \quad \boldsymbol{x} = \boldsymbol{x}' - \boldsymbol{x}'', \ s = t' - t'', \tag{20a}$$

instead of using the corresponding Lagrangian quantities. We denote the $(\boldsymbol{k}, \omega)$-Fourier transform of $W(\boldsymbol{x}, s)$ as $\mathcal{W}(\boldsymbol{k}, \omega)$, i.e., $\mathcal{W}(\boldsymbol{k}, \omega) \equiv \mathcal{F}\{W(\boldsymbol{x}, s)\}$. This is the turbulence kinetic energy TKE density (per unit mass) in the $\boldsymbol{k}$- and ω-spaces simultaneously. In isotropic turbulence, $\mathcal{W}(\boldsymbol{k}, \omega)$ is independent of the direction of $\boldsymbol{k}$, thus $\mathcal{W}(\boldsymbol{k}, \omega) \Rightarrow \mathcal{W}(k, \omega)$. In this case instead of $\mathcal{W}(k, \omega)$, it is convenient to introduce

$$E_{\mathrm{BL}}(k, \omega) \equiv 2\pi k^2 \mathcal{W}(k, \omega), \tag{20b}$$

which is the BL kinetic energy density in *one-dimensionalk*- and frequency ω-space simultaneously. It has the dimensions $\lfloor E_{\mathrm{BL}}(\boldsymbol{k}, \omega) \rfloor = \mathcal{L}^3/\tau$. Furthermore, $E_{\mathrm{BL}}(k, \omega)$ is related to the Eulerian energy spectrum in the k-space, $E_{\mathrm{E}}(k)$, via integrals with respect to the frequency ω according to

$$E_{\mathrm{E}}(k) = \int \frac{\mathrm{d}\omega}{2\pi} E_{\mathrm{BL}}(k, \omega), \tag{21a}$$

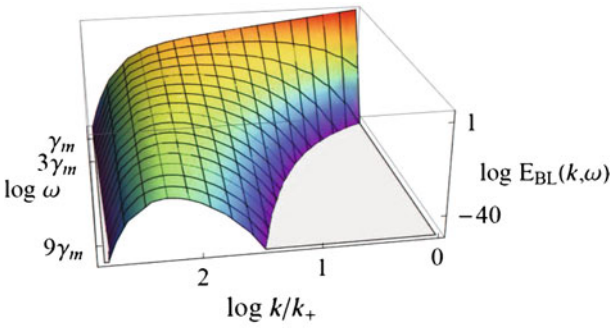

(a) $E_{\mathrm{BL}}(k,\omega)$

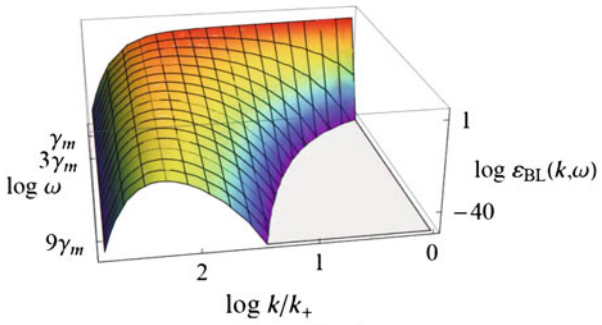

(b) $\varepsilon_{\mathrm{BL}}(k,\omega)$

Fig. 10 3D plots of $E_{\mathrm{BL}}(k,\omega)$ and $\varepsilon_{\mathrm{BL}}(k,\omega)$ according to (23) in which $E_{\mathrm{E}}(k)$ is prescribed as $E_{\mathrm{E}}(k) = k^{-5/3}\exp[-k^2/10^4]$ and $\varepsilon_{\mathrm{E}}(k) = 2k^2 E_{\mathrm{E}}(k)$

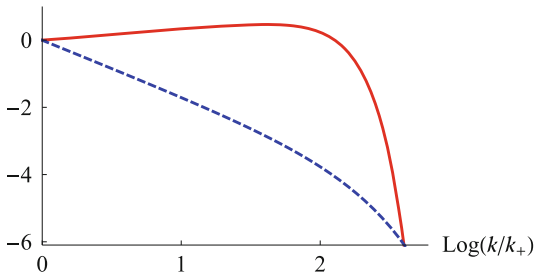

(a) $E_{\mathrm{BL}}(k)$: dashed line, and $\varepsilon_{\mathrm{BL}}(k)$: solid line

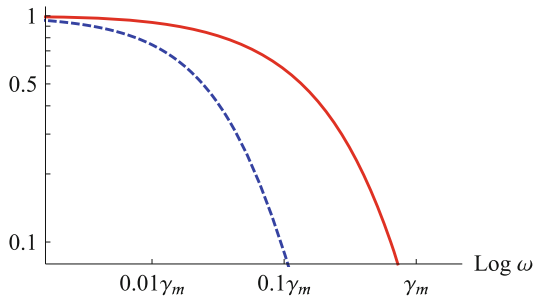

(b) $E_{\mathrm{BL}}(\omega)$: dashed line, and $\varepsilon_{\mathrm{BL}}(\omega)$: solid line

Fig. 11 Plots of the Eulerian and Lagrangian spectra. **a** $E_{\mathrm{BL}}(k)$ and $\varepsilon_{\mathrm{BL}}(k)$ are integrals with respect to ω of the spectra $E_{\mathrm{BL}}(k,\omega)$ and $\varepsilon_{\mathrm{BL}}(k,\omega)$; **b** $E_{\mathrm{BL}}(\omega)$ and $\varepsilon_{\mathrm{BL}}(\omega)$ are integrals with respect to k of $E_{\mathrm{BL}}(k,\omega)$ and $\varepsilon_{\mathrm{BL}}(k,\omega)$

and to $E_{\mathrm{L}}(\omega)$ and $\varepsilon_{\mathrm{L}}(\omega)$ via the k-integrals:

$$E_{\mathrm{L}}(\omega) = \int E_{\mathrm{BL}}(k,\omega)\,\mathrm{d}k, \tag{21b}$$

$$\varepsilon_{\mathrm{L}}(\omega) = 2\nu \int k^2\, E_{\mathrm{BL}}(k,\omega)\,\mathrm{d}k. \tag{21c}$$

In Eq. (21c), we have used the result of [15] that the dissipative term in the balance equation for $\mathcal{W}(\boldsymbol{k},\omega)$ has the simple form $2\nu k^2\mathcal{W}(\boldsymbol{k},\omega)$. The total TKE (per unit mass) can be written as follows:

$$E = \int \frac{\mathrm{d}\omega}{2\pi}\,\mathrm{d}k\; E_{\mathrm{E}}(k) = \int \mathrm{d}k\; E_{\mathrm{E}}(k) = \int \frac{\mathrm{d}\omega}{2\pi}\, E_{\mathrm{L}}(\omega). \tag{22}$$

L'vov and Procaccia [15] have shown that in the BL-reference frame (as well as in the Lagrangian coordinates) the kinematic sweeping of small eddies by the velocity field of the larger eddies is absent, and thus the characteristic frequency for the k-scale motions is $\gamma(k)$. Therefore, in the inertial range of isotropic turbulence, $E_{\mathrm{BL}}(k,\omega)$ is approximated as:

$$E_{\mathrm{BL}}(k,\omega) \approx \frac{2\pi}{\gamma(k)}\,\Phi\left[\frac{\omega}{\gamma(k)}\right]E(k), \tag{23a}$$

where $\int \Phi(x)\,\mathrm{d}x = 1$. The exact form of $\Phi(x)$ is not known. However, [15] indicated that $\mathcal{W}(\boldsymbol{k},\omega)$ decays much faster than $1/x^2$ for $\lim_{x\to\infty}$. For simplicity, we chose:

$$\Phi_1(x) = \exp(-x). \tag{23b}$$

Equations (21) and (23) give:

$$E_{\mathrm{L}}(\omega) \simeq 2\pi \int \Phi\left[\frac{\omega}{\gamma(k)}\right]\frac{E_{\mathrm{E}}(k)\,\mathrm{d}k}{\gamma(k)}, \quad \text{Eulerian–Lagrangian bridge for energy spectra;} \tag{24a}$$

$$\frac{\varepsilon_{\mathrm{L}}(\omega)}{2\nu} \simeq 2\pi \int \Phi\left[\frac{\omega}{\gamma(k)}\right]\frac{k^2 E_{\mathrm{E}}(k)\,\mathrm{d}k}{\gamma(k)}, \quad \text{Eulerian–Lagrangian bridge for dissipation spectra} \tag{24b}$$

Substituting Eq. (23b) in Eq. (24), we got Eq. (13), that culminate our derivation of the bridge relations used in this paper.

Figures 10 and 11 show how the bridge relationships (24) work. Figure 10a displays the 3D-shape of the function $E_{\mathrm{BL}}(k,\omega)$ according to Eq. (23a) in which $\Phi(x)$ is given by Eq. (23b), and $E_{\mathrm{E}}(k)$ is modeled as $E_{\mathrm{E}}(k) = k^{-5/3}\exp[-(k/k_{\max})^2]$, where the dimensionless $k \geq 1$ is normalized by the outer scale of turbulence and the viscous cutoff is chosen as $k_{\max} = 100$. Dimensionless turnover frequency $\gamma(k) = k^{2/3}$ is normalized by that of the outer-scale eddies. Figure 10b shows the 3D-shape of the dissipation $\varepsilon_{\mathrm{BL}}(k,\omega)$ in the k-ω space. Figure 11a shows the Eulerian spectra $E_{\mathrm{BL}}(k)$ and $\varepsilon_{\mathrm{BL}}(k)$ which are the integrals with respect to ω of the spectra $E_{\mathrm{BL}}(k,\omega)$ and $\varepsilon_{\mathrm{BL}}(k,\omega)$. Figure 11b shows the Lagrangian spectra $E_{\mathrm{BL}}(\omega)$ and $\varepsilon_{\mathrm{BL}}(\omega)$ which are integrals with respect to k of $E_{\mathrm{BL}}(k,\omega)$ and $\varepsilon_{\mathrm{BL}}(k,\omega)$.

References

1. Batchelor, G.K.: Diffusion in a field of homogeneous turbulence. ii. The relative motion of particles. Proc. Camb. Philos. Soc. **48**, 345–362 (1952)
2. Belinicher, V.I., L'vov, V.S.: A scale-invariant theory of developed hydrodynamic turbulence. Sov. Phys. JETP **93**, 1269–1280 (1987)
3. Benzi, R., Biferale, L., Fisher, R., Lamb, D.Q., Toschi, F.: Inertial range Eulerian and Lagrangian statistics from numerical simulations of isotropic turbulence. J. Fluid Mech. **653**, 221–224 (2010)
4. Corrsin, S.: Estimates of the relations between Eulerian and Lagrangian scales in large Reynolds number turbulence. J. Atmos. Sci. **20**, 115–119 (1963)
5. Ferrante, A.: Reduction of Skin Friction in a Microbubble-Laden Spatially-Developing Turbulent Boundary Layer Over a Flat Plate. Ph.D. Thesis. University of California, Irvine (2004)
6. Gkioulekas, E.: On the elimination of the sweeping interactions from theories of hydrodynamic turbulence. Physica D **226**, 151–172 (2007)
7. Hinze, J.O.: Turbulence. McGraw-Hill, New York (1975)
8. Khan, M.A.I., Vassilicos, J.C.: A new Eulerian–Lagrangian length-scale in turbulent flows. Phys. Fluids **16**, 216–218 (2004)
9. Kolmogorov, A.N.: The local structure of turbulence in an incompressible viscous fluid for very large Reynolds numbers. Dokl. Akad. Nauk SSSR **30**, 303–313; reprinted in Proc. R. Soc. Lond. A **434**, 9–13 (1991), 1941
10. Kraichnan, R.H.: The structure of isotropic turbulence at very high Reynolds number. J. Fluid Mech. **5**, 497–543 (1959)
11. Kraichnan, R.H.: Lagrangian-history closure approximation for turbulence. Phys. Fluids **20**, 575–598 (1965) (and erratum 9, 1966, 1884)
12. Kraichnan, R.H.: Eulerian and Lagrangian renormalization in turbulence theory. J. Fluid Mech. **83**, 349–374 (1977)
13. Lucci, F., Ferrante, A., Elghobashi, S.: Modulation of isotropic turbulence by particles of Taylor-lengthscale size. J. Fluid Mech. **650**, 5–55 (2010)
14. Lundgren, T.S.: Linearly forced isotropic turbulence. pp. 461–473. Annual Research Briefs, Center for Turbulence Research, Stanford (2003)
15. L'vov, V.S., Procaccia, I.: Exact resummations in the theory of hydrodynamic turbulence: I. The ball of locality and normal scaling. Phys. Rev. E **52**, 3840–3857 (1995)
16. Martin, P.C., Siggia, E.D., Rose, H.A.: Statistical dynamics of classical systems. Phys. Rev. A **8**, 423–437 (1973)

17. Monin, A.S.: The theory of locally isotropic turbulence. Dokl. Akad. Nauk. SSSR **125**, 515–518 (1959)
18. Pope, S.B.: Turbulent Flows. Cambridge Univ Press (2000)
19. Richardson, L.F.: Atmospheric diffusion shown on a distance-neighbour graph. Proc. R. Soc. Lond. A **110**, 709–737 (1926)
20. Taylor, G.I.: Diffusion by continuous movement. Proc. Lond. Math. Soc. A **20**, 196 (1921)
21. Tennekes, H.: Eulerian and Lagrangian time microscales in isotropic turbulence. J. Fluid Mech. **67**, 561–567 (1975)
22. Tennekes, H., Lumley, J.L.: A First Course in Turbulence. The MIT Press, Cambridge, MA (1972)
23. Wyld, H.W.: Formulation of the theory of turbulence in an incompressible fluid. Ann. Phys. **14**, 143–165 (1961)
24. Yeung, P.K.: Lagrangian investigations of turbulence. Annu. Rev. Fluid Mech. **34**, 115–142 (2002)